JACS
JOURNAL OF THE AMERICAN CHEMICAL SOCIETY

Article

pubs.acs.org/JACS


# How Light-Harvesting Semiconductors Can Alter the Bias of Reversible Electrocatalysts in Favor of $H_2$ Production and $CO_2$ Reduction

Andreas Bachmeier,[†] Vincent C. C. Wang,[†] Thomas W. Woolerton,[†] Sophie Bell,[†] Juan C. Fontecilla-Camps,[‡] Mehmet Can,[§] Stephen W. Ragsdale,[§] Yatendra S. Chaudhary,*[,†,∥] and Fraser A. Armstrong*[,†]

[†]Inorganic Chemistry Laboratory, Department of Chemistry, University of Oxford, South Parks Road, Oxford OX1 3QR, Oxfordshire, United Kingdom

[‡]Laboratoire de Cristallographie et Cristallogenèse des Proteines, Institut de Biologie Structurale Jean-Pierre Ebel: CEA/CNRS, Université Joseph Fourier, 38041 Grenoble cedex 9, Rhône-Alpes, France

[§]Department of Biological Chemistry, University of Michigan, Ann Arbor, Michigan 48109-0606, United States

[∥]Colloids and Materials Chemistry Department, CSIR-Institute of Minerals and Materials Technology, Bhubaneswar, Odisha 751013, India

Supporting Information

**ABSTRACT:** The most efficient catalysts for solar fuel production should operate close to reversible potentials, yet possess a bias for the fuel-forming direction. Protein film electrochemical studies of Ni-containing carbon monoxide dehydrogenase and [NiFeSe]-hydrogenase, each a reversible electrocatalyst, show that the electronic state of the electrode strongly biases the direction of electrocatalysis of $CO_2$/CO and $H^+/H_2$ interconversions. Attached to graphite electrodes, these enzymes show high activities for both oxidation and reduction, but there is a marked shift in bias, in favor of $CO_2$ or $H^+$ reduction, when the respective enzymes are attached instead to n-type semiconductor electrodes constructed from CdS and $TiO_2$ nanoparticles. This catalytic rectification effect can arise for a reversible electrocatalyst attached to a semiconductor electrode if the electrode transforms between semiconductor- and metallic-like behavior across the same narrow potential range (<0.25 V) that the electrocatalytic current switches between oxidation and reduction.

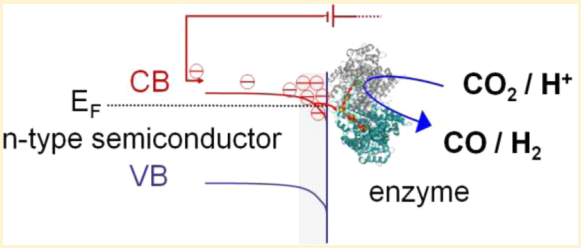


## INTRODUCTION

In artificial photosynthesis (AP), a research area that falls within the active and important realm of "renewable energy/solar fuels", the fuel- or $O_2$-forming catalysts attached to a light absorber (e.g., semiconductor) can be regarded as electrocatalysts since they catalyze the respective electrochemical half cell reactions. Ideal AP catalysts should exhibit high activity and not require a large, wasteful overpotential to drive the reaction; however, a minimal overpotential requirement corresponds most closely to reversibility, whereas it is beneficial to render the reaction as unidirectional as possible, thus trapping the electron or hole and opposing recombination.[1] Under the condition of low overpotential that is beneficial for efficiency, it is interesting and important to consider how the relative rates of catalysis for forward and reverse directions can be biased in favor of the desired direction.

In principle, such a bias can be provided if the carrier density of the semiconductor material changes substantially within a potential region close to the reduction potential of the reaction of interest. Electrochemical kinetics at semiconductors depend on the density of charge carriers in the space-charge region adjacent to the solution interface.[2,3] A useful physical characteristic of a semiconductor, unrestricted by its chemical nature, but of general relevance, is the flatband potential ($E_{FB}$). For an n-type semiconductor, as the applied potential becomes more negative than $E_{FB}$, the increasing electron density at the surface gives rise to an accumulation layer; the conduction and valence bands bend downward and the semiconductor approaches metallic-like behavior. In contrast, when the applied potential is increased relative to $E_{FB}$, a depletion layer forms and the bands bend upward, resulting in a barrier for electron transfer from the catalyst to the semiconductor. At $E_{FB}$ there is no band bending. The space-charge region may extend well into the material (values in the range 10 nm to 1 $\mu$m being reported).[2]

For $H_2$ production, platinum is well established as a reversible catalyst, but it could never be scaled up for large-area AP, and there is much interest in finding alternatives. For $CO_2$ reduction, there are no examples of *reversible* catalysts

**Received:** April 29, 2013
**Published:** September 26, 2013

   dx.doi.org/10.1021/ja4042675 | J. Am. Chem. Soc. 2013, 135, 15026−15032

based on materials or small molecules. Although a variety of catalysts are being explored to drive $H^+/CO_2$ reduction to fuels,[4−7] the high overpotential requirements and/or low turnover rates command much room for improvement. In contrast, many enzymes are now known to behave as *reversible* electrocatalysts, particularly those catalyzing $H^+$ and $CO_2$ reduction,[8,9] and they are valuable models for understanding electrocatalysis at a more fundamental level. The buried active site of an enzyme is much less likely to be perturbed by the nature of the electrode material than a small molecule catalyst. Since an enzyme has specialized parts (long-range electron transfer and storage, substrate/product transport, catalysis by inner-sphere proton-coupled electron transfers) the component steps of electrocatalysis can be resolved, often exploiting genetic engineering of the enzyme structure. Two particular classes of enzyme have been extensively studied by protein film electrochemistry (PFE): hydrogenases ($H_2$ase) and carbon monoxide dehydrogenases (CODH) each possess highly active Fe- and Ni-containing active sites and exhibit turnover frequencies often measured in thousands ($10^3$−$10^4$) per second at minimal overpotential, achieving $H^+$ and $CO_2$ reduction at −0.45 to −0.55 V vs SHE under neutral aqueous conditions.[10−12]

Several reports have described the electrochemistry of proteins on semiconductor electrodes. Durrant et al. reported a series of studies dealing with the electrochemistry of cytochrome *c* and hemoglobin immobilized on $TiO_2$ film electrodes.[13,14] They found irreversible reduction of the proteins' active sites at potentials substantially more negative than the solution-based redox potentials, similar to observations with simple redox couples such as potassium ferricyanide $K_3[Fe(CN)_6]$.[14] The $TiO_2$ electrode thus exerts a rectifying effect: however, these electrochemical reductions are not catalytic.

We now explore the directionality that can be imposed on electrocatalytic behavior when certain enzymes and, by extension, any *reversible* electrocatalysts are attached to a semiconductor (Figure 1). Although materials will differ considerably in their chemical properties, the concept of $E_{FB}$ provides a useful reference point. Since a reversible electrocatalytic reaction changes direction across a small potential region, the effect of a change in carrier density across this region should be particularly influential. We have therefore compared the reversibility of $H^+/H_2$ and $CO_2/CO$ interconversion by $H_2$ase and CODH at a metallic-like graphite electrode and at $TiO_2$ and CdS electrodes (n-type semiconductors) by analyzing the electrocatalytic voltammograms recorded under $H_2$ or $CO_2$/CO mixtures.

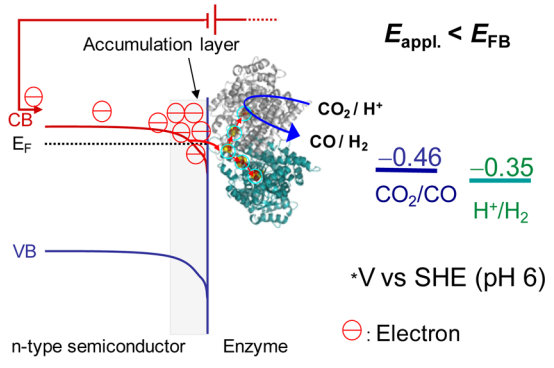


**Figure 1.** Schematic representation of the formation of an accumulation layer at the surface of CdS or $TiO_2$ due to the increased electron density at the surface when $E_{appl}$ is lowered relative to $E_{FB}$. The increased electron density and subsequent downward band bending facilitate efficient electron transfer to the enzyme active site via FeS clusters to catalyze $H_2$ production or $CO_2$ reduction. The term $E_F$ is the Fermi energy level of the semiconductor.

We studied the [NiFeSe]-$H_2$ase (henceforth, simply $H_2$ase) from *Desulfomicrobium baculatum* (the "Se" refers to the fact that one of the cysteine ligands normally coordinating the Ni is replaced by selenocysteine) and CODH I (henceforth, simply CODH) from *Carboxydothermus hydrogenoformans*, which has a [Ni4Fe-4S] active site. These enzymes contain electron-transfer relays comprised of FeS clusters,[15,16] and when attached to a metallic electrode (including pyrolytic graphite, a semimetal), they are excellent examples of reversible electrocatalysts.[8,17−20] Voltammograms of a solution containing both oxidized and reduced forms of the substrate (the redox-active molecules in solution) intersect the zero current axis at the equilibrium potential with little or no inflection.

The electrocatalytic behavior of each enzyme was compared on three different materials: graphite, and CdS and $TiO_2$ (both n-type semiconductors). The conduction band potentials of CdS and anatase ($E_{CB}$ at ca. −0.87 and ca. −0.52 V vs SHE, pH 6, respectively)[21] are more negative than the equilibrium potentials for $H^+/H_2$ (−0.36 V vs SHE) and $CO_2/CO$ (−0.46 V), and nanoparticles of CdS and dye-sensitized $TiO_2$ (anatase or P25, a mixed rutile-anatase phase) modified by attaching $H_2$ase or CODH have been shown to be excellent systems for photoreducing $H_2O$ and $CO_2$.[11,12,22−24]

## MATERIALS AND METHODS

Synthesized porous thin films of hexagonal phase CdS and $TiO_2$ (Degussa P25) on indium tin oxide (ITO; Supporting Information) and fluorine doped tin oxide (FTO) were converted into electrodes by making an ohmic contact with Cu wire on the uncoated area of the conducting glass and sealed with nonconducting epoxy (Figure 2 and Supporting Information, Figure S2).

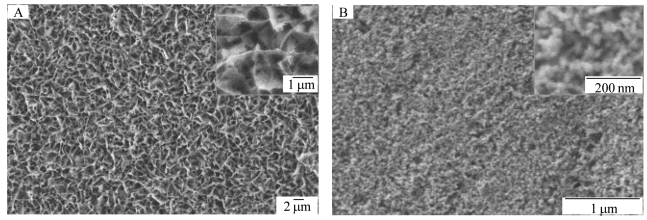


**Figure 2.** SEM images of CdS (A) and $TiO_2$ (B) film electrodes. The scale bars are (A) 2 and 1 μm (inset) and (B) 1 μm and 200 nm (inset).

The CdS thin film consists of a highly porous 3-dimensional network of CdS nanoflakes/sheets. These nanosheets are typically 20 ± 5 nm in width. The pore size of CdS varies from 700 nm to approximately 1 μm. The $TiO_2$ thin film exhibits porous structures consisting of nanoparticles (of the order of 20 nm), which have formed aggregates, as expected upon calcination at 450 °C. Pyrolytic graphite "edge" (PGE, Figure S1, Supporting Information) electrodes of geometric surface area 0.03 $cm^2$ were constructed in house as described previously.[25]

To study the electrocatalytic behavior of the enzymes on CdS, $TiO_2$, and PGE, aliquots of enzyme samples (either CODH or $H_2$ase, <10 pmol) were drop cast onto the electrode and left for a few minutes until partially dry. In the case of PGE, the electrode was abraded using P400 Tufbak Durite sandpaper and sonicated to remove carbon debris before attachment of enzyme. The electrode was then


dx.doi.org/10.1021/ja4042675 | J. Am. Chem. Soc. 2013, 135, 15026−15032

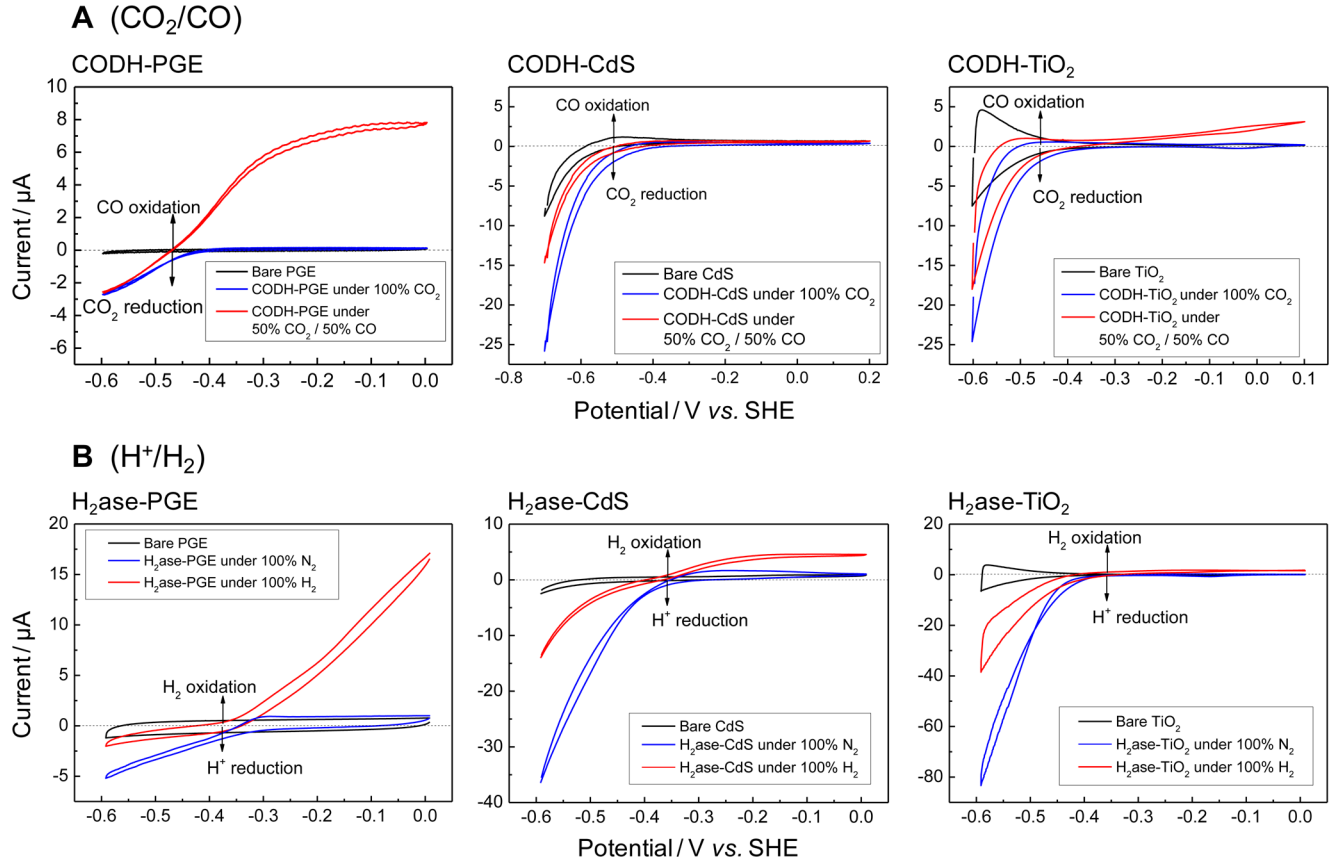


**Figure 3.** Cyclic voltammograms (10 mV $s^{-1}$) of unmodified (black) and enzyme-modified electrodes (red, blue), 0.2 M MES, pH 6.0, 20 °C. Voltammograms recorded under 100% $CO_2$ (CODH-PGE, CODH-CdS and CODH-$TiO_2$) or 100% $N_2$ ($H_2$ase-PGE, $H_2$ase-CdS and $H_2$ase-$TiO_2$) are depicted in blue. Experiments in a 50% $CO_2$/50% CO gas mixture (CODH-PGE, CODH-CdS and CODH-$TiO_2$) bubbling through the cell or with 100% $H_2$ bubbling through the cell ($H_2$ase-PGE, $H_2$ase-CdS, and $H_2$ase-$TiO_2$) are shown in red.

placed in an electrochemical cell and used as the working electrode with Ag/AgCl (1 M KCl) as reference and Pt wire as counter. All potentials are quoted vs the standard hydrogen electrode (SHE) using the conversion $E_{SHE} = E_{Ag/AgCl} + 234$ mV at 20 °C. The electrolyte was 0.2 M MES at pH 6.0, and all solutions were prepared using purified water (Millipore, 18 MΩ cm). Electrochemical measurements were made with an Autolab potentiostat (PGSTAT30) controlled by Nova software (EcoChemie). Impedance measurements were conducted using an Ivium Technologies COMPACTSTAT.e portable electrochemical interface and impedance analyzer, controlled by IviumSoft software. Cyclic voltammograms were recorded prior to and after impedance and chronoamperometric experiments with enzyme-modified electrodes, in order to ensure that the catalytic activity of the enzyme had remained steady throughout the measurements. Precise gas mixtures (BOC gases) were created using mass flow controllers (Sierra Instruments), and the electrochemical cell was constantly purged with the gas mixture throughout the experiments. Because of the oxygen sensitivity of the enzymes, all experiments were performed inside an anaerobic glovebox (Belle Technologies, $O_2$ < 3 ppm) and in the dark, unless otherwise stated.

Isolation, purification and activity measurements of CODH I from *Carboxydothermus hydrogenoformans* were carried out according to previously described procedures.[26] The activity for CO oxidation was 1300 μmol $min^{-1}$ $mg^{-1}$ at 20 °C. The [NiFeSe]-hydrogenase sample from *Desulfomicrobium baculatum* was obtained according to previously published methods.[20,27] The specific $H_2$ oxidation activity of the $H_2$ase was determined as 1700 μmol $min^{-1}$ $mg^{-1}$, using conventional room-temperature assays after a few minutes under $H_2$ to fully activate the enzyme. Chronoamperometry experiments depicting the stability of CODH and $H_2$ase on the three different electrode materials used in this report are shown in Figure S3 (Supporting Information).

## RESULTS AND DISCUSSION

Row A of Figure 3 shows cyclic voltammograms (CVs) of CODH attached to PGE (CODH-PGE), CdS (CODH-CdS), and $TiO_2$ (CODH-$TiO_2$) in separate experiments with 100% $CO_2$ or a mixture of 50% $CO_2$/50% CO gently bubbling through the cell solution. The catalytic current is directly related to the rate of catalysis in either direction. A positive current corresponds to substrate oxidation, and a negative current corresponds to reduction. Rather than reporting current densities, we display current vs voltage curves in this report: in PFE it is rarely possible to ascertain the electroactive coverage of enzyme as this requires the detection and integration of reversible signals (for example, due to FeS redox couples), which are usually vanishingly small. It is the high activity of enzymes that amplifies the current. Instead, PFE provides precise and continuous measurement of the *relative* catalytic rates in either direction. Importantly, the shapes of the CVs on PGE in the presence of both the oxidized and reduced substrates reveal the inherent catalytic bias of the enzymes to function more effectively in one particular direction. A dominant factor in determining the bias of an enzyme is the reduction potential ($E^0_{Ox/R}$) of the relay center of the enzyme that serves as the electron entry/exit point for transfer to the buried catalytic center.[9]


dx.doi.org/10.1021/ja4042675 | J. Am. Chem. Soc. 2013, 135, 15026−15032

In contrast to CODH at PGE, the voltammograms for the CODH-CdS and CODH-$TiO_2$ electrodes are dominated by $CO_2$ reduction (vide infra); i.e., the bias appears *reversed* (with respect to the bias observed at PGE) to favor instead the formation of CO; in fact CO oxidation is negligible at CdS and extremely sluggish at $TiO_2$. The effect is all the more pronounced if we consider that CO is a natural inhibitor of $CO_2$ reduction by CODH (product inhibition);[28] i.e., the exponentially increasing reductive current is suppressed when both oxidized and reduced substrate is present. Voltammograms recorded under 100% $CO_2$ reveal the further increase in current that is obtained when CO is not introduced.

Row B shows analogous experiments for $H_2$ase on PGE, CdS and $TiO_2$ while $H_2$ is gently bubbled through the cell solution. Once again, the effect of product inhibition is clearly visible in the case of $H_2$ase-PGE.[20] Electrocatalysis in the reduction direction is strongly inhibited by $H_2$, whereas CVs recorded in the absence of $H_2$ reveal the higher rate of $H^+$ reduction by uninhibited enzyme. As with CODH, comparison with PGE shows that the $H_2$ oxidation currents at CdS or $TiO_2$ are greatly suppressed relative to the rates of $H^+$ reduction.

The potential dependencies of the low-level CO and $H_2$ oxidation currents at CdS and $TiO_2$ varied slightly between different experiments: this scatter is most likely due to nonidealities such as dispersion in interactions between enzyme and semiconductor surface and direct contact between some enzyme molecules and the conducting oxide support. Typical ratios of currents for reduction vs oxidation are shown graphically in Figure S4 (Supporting Information). Comparing background-subtracted oxidation and reduction currents at ±0.15 V either side of the thermodynamic potential for $CO_2$/CO and $H^+/H_2$ interconversion (Figure 3) clearly reveals the changes in catalytic bias for each enzyme. For $H_2$ase the current ratio ($H_2$ oxidation/$H^+$ reduction) drops from 8.1 on PGE to 0.81 (CdS) and 0.11 ($TiO_2$), i.e., attenuation factors of approximately 10- and 80-fold, respectively. For CODH the current ratio (CO oxidation/$CO_2$ reduction) drops from 2.2 (PGE) to 0.04 (CdS) and 0.05 ($TiO_2$), i.e., an attenuation factor of approximately 50-fold in each case. These results demonstrate that although the residual oxidizing currents for both enzymes differ at $TiO_2$ and CdS, the oxidation reactions are essentially rendered irreversible.

Previously, we reported photoinduced $CO_2$ reduction using CODH-$TiO_2$ and CODH-CdS nanoassemblies comprising the respective nanoparticles and enzymes we have now used in this work.[12,23] Using gas chromatography, we were able to monitor the catalytic reduction of $CO_2$ to CO. In this work we used instead a selective inhibitor of CODH to prove that the reduction currents at each electrode correspond to the catalytic conversion of $CO_2$ into CO. We recently established that cyanate ($NCO^-$), an isoelectronic $CO_2$ analogue, targets the active site of CODH by intercepting the reduced $C_{red2}$ level and blocking $CO_2$ reduction.[28] Cyanate is released as the potential is raised and does not significantly inhibit CO oxidation.

Figure 4 depicts the selective and quantitative inhibition of $CO_2$ reduction on CODH-modified $TiO_2$ and CdS electrodes after adding KOCN to a final concentration of 20 mM to CODH-$TiO_2$ (Figure 4A) and 60 mM to CODH-CdS (Figure 4B). The portions of the cathodic currents due to $CO_2$ reduction (before introducing the inhibitor, blue traces) are quenched. Instead, for CODH-$TiO_2$, the voltammogram resembles the characteristic shape of a $TiO_2$ electrode at low potential. In the CODH-CdS system, the voltammogram also

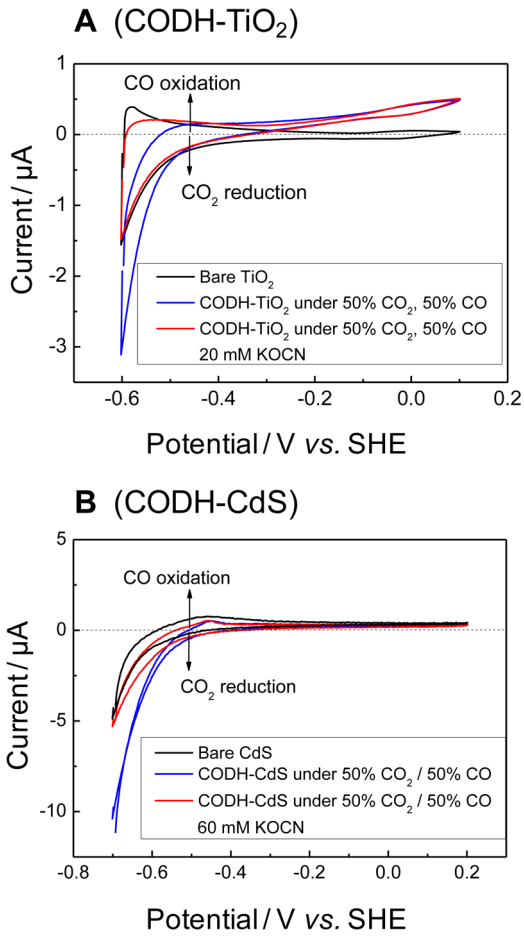


**Figure 4.** Cyclic voltammograms showing selective inhibition of $CO_2$ reduction on CODH-modified $TiO_2$ (A) and CdS (B) in the presence of 20 and 60 mM KOCN, respectively, under a mixture of 50% $CO_2$, 50% CO bubbling through the cell. Solutions contained 0.2 M MES (pH 6.0); temperature 20 °C; scan rate 10 mV $s^{-1}$.

closely resembles the shape of the bare electrode after introduction of the inhibitor. We thus establish that the reductive catalytic current stems specifically from $CO_2$ reduction.

For $TiO_2$, the increase in reduction current for both $H^+$ and $CO_2$ coincides closely with the trumpet-shaped increase in electrode charging current that is observed in the blank experiments.[29,30] In chemical terms, the background waveshape can be ascribed to the reversible reduction of $Ti^{4+}$ surface centers,[29] the effect of which is to increase the carrier density as the potential is lowered. An analogous observation is not apparent for CdS, so to obtain more insight we carried out impedance experiments in order to measure how the capacitance varies with potential and thus gain an estimate of $E_{FB}$ under different conditions. The flatband potential ($E_{FB}$) values for CdS and $TiO_2$ were determined to be ca. −0.61 and ca. −0.50 V vs SHE, respectively, from Mott−Schottky plots of capacitance data at 1 kHz (Figure 5A and B).[3,31] The value measured for $TiO_2$ at pH 6.0/20 °C agrees well with the value of −0.52 V vs SHE predicted by a model for nanostructured $TiO_2$ electrodes in aqueous solution, given by eq 1.[32]

$$E_{FB}(\text{V, SCE}) = -0.40 - (0.06 \times \text{pH}) \quad (1)$$

Mott−Schottky plots recorded on $TiO_2$ electrodes in a different protic electrolyte solution confirmed that the flatband


dx.doi.org/10.1021/ja4042675 | J. Am. Chem. Soc. 2013, 135, 15026−15032

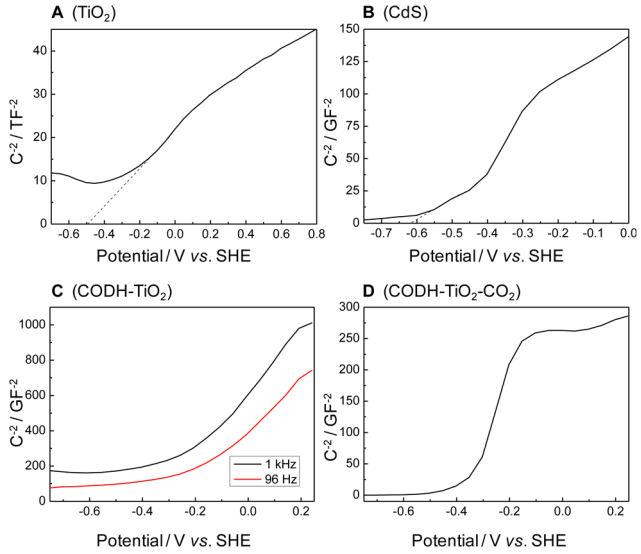


**Figure 5.** Mott–Schottky plots ($1/C^2$ vs Potential) recorded at 20 °C, 1 kHz for (A) $TiO_2$, (B) CdS, (C) CODH-$TiO_2$, and (D) CODH-$TiO_2$ in the presence of $CO_2$. Each plot was measured at 1 kHz under 100% $N_2$ apart from (D), which was measured at 78 Hz under 100% $CO_2$. The cell buffer solution was 0.2 M MES (pH 6.0) in all experiments.

potential is independent of the electrolyte;[32] i.e., the capacitance of the Helmholtz layer at the semiconductor–electrolyte interface is negligible compared to the capacitance of the space-charge region (Figure S5, Supporting Information). Two further experiments were carried out with $TiO_2$ in the presence of CODH, first under "nonturnover" conditions, i.e., under 100% $N_2$ without the presence of substrate (Figure 5C; an equivalent experiment on CODH-CdS is shown in the Supporting Information, Figure S5) and then under 100% $CO_2$ (Figure 5D). Analogous "substrate free" impedance experiments could not be conducted using $H_2$ase, as protons of the buffer solution constitute the substrate. The experiments showed that the presence of enzyme alone has a considerable effect on the shape of the Mott–Schottky plot (Figure 5C) and revealed an interesting effect when substrate is added (Figure 5D). The experiment carried out in the presence of enzyme alone shows an unfeatured shape at mid-to-low frequencies, whereas the much sharper plot obtained in the presence of $CO_2$ (yielding $E_{FB} = -0.59$ V) becomes flattened as the frequency is raised. Although the SEM image in Figure 2A shows the pores in the $TiO_2$ film to be of approximately the same size as the dimensions of CODH (approximately 88 × 63 × 60 Å), our observations suggest the enzyme adsorbs on the outer surface and acts mainly as a resistive film. However, when $CO_2$ is introduced, a charge-transport pathway becomes available and a flatband potential can be measured at low frequencies that allow electron transfer and catalysis to occur. These experiments are at a preliminary stage and suggest important possibilities for using impedance techniques to study catalytic electron transfer in enzymes.

Semiconductor nanoparticles and highly porous nanocrystalline electrodes are considered to be too small to support an effective space-charge region due to the very small crystallite sizes.[33] In contrast, the $TiO_2$ particles in our nanocrystalline films are interconnected and partly fused together (Figure 2). Studies on similarly structured $TiO_2$ electrodes suggest that the electronic properties of such aggregates are not completely dominated by the individual particles but instead exhibit bulk properties to some extent, rendering the formation of a space-charge layer possible.[34]

The results depicted in Figure 3 clearly display a pronounced rectification of the otherwise reversible electrocatalysis of $H^+/H_2$ and $CO_2/CO$ interconversion by enzymes, when measured at $TiO_2$ and CdS electrodes instead of PGE. According to established models, the surface concentration of electrons (the majority carrier for an n-type semiconductor) increases exponentially as the potential is lowered: it is controlled, through a Boltzmann-like relationship, by the difference between $E_{FB}$ and the applied potential.[35] As the electrode potential is lowered through $E_{FB}$, there is a transformation to metallic-like character as an accumulation layer forms (Figure 1): the increase in electron density at the semiconductor-catalyst interface favors efficient electron transfer from the semiconductor to the enzyme to drive reduction. In contrast, raising the applied potential above $E_{FB}$ results in a depletion layer that poses a barrier for electron transfer from the enzyme to the semiconductor. This reasoning explains the resistive effect observed for the oxidation reactions when enzymes are coupled on CdS and $TiO_2$ surfaces. The $E_{FB}$ values broadly lie within 0.25 V of the reduction potentials for $CO_2/CO$ and $H^+/H_2$ under the experimental conditions used: this is important because the catalysts are operating in a nearly reversible manner and the respective currents change direction (oxidation ↔ reduction) across the same limited potential region. The apparent catalytic bias of each enzyme is thus shifted to favor fuel formation when coupled to CdS and $TiO_2$ electrode surfaces.

Finally, we studied visible-light-driven $H_2$ production at the $H_2$ase-CdS electrode, as CdS has a band gap of around 2.3 eV (540 nm). Cyclic voltammograms were first recorded on an unmodified (bare CdS) electrode, both in the dark and under illumination ($\lambda$ > 420 nm, intensity 16 mW $cm^{-2}$). To eliminate heating effects, the bath temperature was monitored during experiments, and no light-dependent variation was noted. Upon irradiation, the unmodified CdS electrode exhibits an anodic photocurrent (as expected for an n-type semiconductor at a potential positive of $E_{FB}$) at potentials above −0.4 V, Figure 6A. In experiments performed on $H_2$ase-CdS under illumination, direct contact of enzyme and the transparent conducting oxide layer does not contribute to the observed photo-oxidation current under light exposure, because ITO is transparent under visible-light irradiation.

Interestingly, under irradiation, the $H^+$ reduction current is further enhanced by photoexcitation of electrons from the valence band into the conduction band, from where they transfer to $H_2$ase, and there is a small but noticeable shift in onset potential. For an n-type semiconductor, at potentials far more negative than $E_{FB}$, illumination should have no effect on the reductive current because the electrode behaves like a metal. In contrast, at potentials closer to $E_{FB}$, illumination can enhance the concentration of electrons available for transfer to the enzyme; the result thus provides further evidence that this factor is important. The observation highlights the importance of the enzyme as a reversible catalyst as the availability (concentration) of electrons can be at least as important as the overpotential driving the reaction.

## ■ CONCLUSIONS

Our results demonstrate that semiconducting electrodes can be used to impose directionality on reversible catalysts that


dx.doi.org/10.1021/ja4042675 | J. Am. Chem. Soc. 2013, 135, 15026–15032

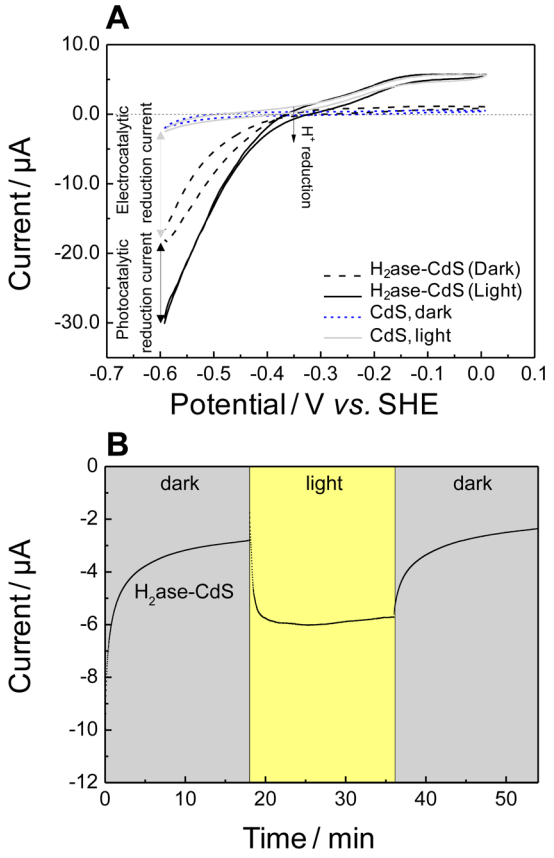


**Figure 6.** (A) Cyclic voltammograms recorded under an inert atmosphere, both under dark conditions and with visible light irradiation ($\lambda$ > 420 nm), for an unmodified CdS electrode, and following modification with $H_2$ase. Scan rate 10 mV $s^{-1}$. (B) Chronoamperometry experiments comparing the catalytic $H_2$ evolution current of $H_2$ase-CdS in the dark and under irradiation at −0.65 V vs SHE. The cell solution was 0.2 M MES (pH 6.0) at 20 °C in both experiments.

operate in the region of the flatband potential. The catalytic direction shifts in response to the (ideally) exponential increase in surface electron concentration that occurs as the potential is changed, thereby, in the case of an n-type semiconductor, favoring reduction over oxidation. This principle of rectifying catalysis provides further design criteria for artificial systems that convert light into storable chemical energy. The enzymes are so proficient that the current is controlled more by the charge carrier availability in the semiconductor than by properties of the catalyst. Although the enzymes used in this work are wholly unsuited for long-term, large-scale systems, our results provide valuable insight for developing integrated artificial systems (based ultimately on abundant chemical catalysts) where getting as close as possible to reversible catalysis is important for efficiency.

## ■ ASSOCIATED CONTENT

### Supporting Information

Full materials and methods, the SEM image of PGE, XRD pattern for CdS and $TiO_2$, chronoamperometry experiments and background-corrected voltammograms for CODH and [NiFeSe]-$H_2$ase coupled to PGE, CdS, and $TiO_2$ electrodes, Mott−Schottky plots for $TiO_2$ recorded in a different electrolyte solution and with CODH adsorbed on CdS. This material is available free of charge via the Internet at http://pubs.acs.org.

## ■ AUTHOR INFORMATION

### Corresponding Author

fraser.armstrong@chem.ox.ac.uk; yschaudhary@immt.res.in

### Notes

The authors declare no competing financial interest.

## ■ ACKNOWLEDGMENTS

The authors thank BBSRC (Grants H003878-1 and BB/I022309), EPSRC (Supergen 5), the European Commission Marie Curie Programme (PIIF-GA-2009-253602), and NIH (GM39451) for supporting research on enzymes in energy technologies. A.B. acknowledges St. John's College Oxford for a St. John's College Graduate Scholarship. V.W. acknowledges the Ministry of Education, Taiwan (R.O.C.), for a studying abroad scholarship. J.C.F.-C. thanks the Agence Nationale de la Recherche. F.A.A. is a Royal Society-Wolfson Research Merit Award holder. We are also grateful to Dr. J. H. Warner of the Department of Materials, University of Oxford, for SEM analysis and Dr. Thomas Esterle for help and discussions on impedance measurements.

## ■ REFERENCES

(1) Soo, H. S.; Agiral, A.; Bachmeier, A.; Frei, H. *J. Am. Chem. Soc.* **2012**, *134*, 17104.
(2) Bott, A. *Curr. Sep.* **1998**, *3*, 87.
(3) Gelderman, K.; Lee, L.; Donne, S. W. *J. Chem. Educ.* **2007**, *84*, 685.
(4) Helm, M. L.; Stewart, M. P.; Bullock, R. M.; DuBois, M. R.; DuBois, D. L. *Science* **2011**, *333*, 863.
(5) Reece, S. Y.; Hamel, J. A.; Sung, K.; Jarvi, T. D.; Esswein, A. J.; Pijpers, J. J. H.; Nocera, D. G. *Science* **2011**, *334*, 645.
(6) Barton, E. E.; Rampulla, D. M.; Bocarsly, A. B. *J. Am. Chem. Soc.* **2008**, *130*, 6342.
(7) Benson, E. E.; Kubiak, C. P.; Sathrum, A. J.; Smieja, J. M. *Chem. Soc. Rev.* **2009**, *38*, 89.
(8) Armstrong, F. A.; Hirst, J. *Proc. Natl. Acad. Sci. U. S. A.* **2011**, *108*, 14049.
(9) Hexter, S. V.; Grey, F.; Happe, T.; Climent, V.; Armstrong, F. A. *Proc. Natl. Acad. Sci. U. S. A.* **2012**, *109*, 11516.
(10) Brown, K. A.; Wilker, M. B.; Boehm, M.; Dukovic, G.; King, P. W. *J. Am. Chem. Soc.* **2012**, *134*, 5627.
(11) Reisner, E.; Powell, D. J.; Cavazza, C.; Fontecilla-Camps, J. C.; Armstrong, F. A. *J. Am. Chem. Soc.* **2009**, *131*, 18457.
(12) Woolerton, T. W.; Sheard, S.; Reisner, E.; Pierce, E.; Ragsdale, S. W.; Armstrong, F. A. *J. Am. Chem. Soc.* **2010**, *132*, 2132.
(13) Topoglidis, E.; Campbell, C.; Cass, A. G.; Durrant, J. R. *Langmuir* **2001**, *17*, 7899.
(14) Topoglidis, E.; Lutz, T.; Durrant, J. R.; Palomares, E. *Bioelectrochemistry* **2008**, *74*, 142.
(15) Garcin, E.; Vernede, X.; Hatchikian, E. C.; Volbeda, A.; Frey, M.; Fontecilla-Camps, J. C. *Structure* **1999**, *7*, 557.
(16) Dobbek, H.; Svetlitchnyi, V.; Gremer, L.; Huber, R.; Meyer, O. *Science* **2001**, *293*, 1281.
(17) Jones, A. K.; Sillery, E.; Albracht, S. P. J.; Armstrong, F. A. *Chem. Commun.* **2002**, 866.
(18) Frey, M. *ChemBioChem* **2002**, *3*, 153.
(19) Parkin, A.; Seravalli, J.; Vincent, K. A.; Ragsdale, S. W.; Armstrong, F. A. *J. Am. Chem. Soc.* **2007**, *129*, 10328.
(20) Parkin, A.; Goldet, G.; Cavazza, C.; Fontecilla-Camps, J. C.; Armstrong, F. A. *J. Am. Chem. Soc.* **2008**, *130*, 13410.
(21) Grätzel, M. *Nature* **2001**, *414*, 338.
(22) Reisner, E.; Fontecilla-Camps, J. C.; Armstrong, F. A. *Chem. Commun.* **2009**, 550.

(23) Woolerton, T. W.; Sheard, S.; Pierce, E.; Ragsdale, S. W.; Armstrong, F. A. *Energy Environ. Sci.* **2011**, *4*, 2393.
(24) Chaudhary, Y. S.; Woolerton, T. W.; Allen, C. S.; Warner, J. H.; Pierce, E.; Ragsdale, S. W.; Armstrong, F. A. *Chem. Commun.* **2012**, *48*, 58.
(25) Sucheta, A.; Cammack, R.; Weiner, J.; Armstrong, F. A. *Biochemistry* **1993**, *32*, 5455.
(26) Seravalli, J.; Ragsdale, S. W. *Biochemistry* **2008**, *47*, 6770.
(27) Hatchikian, E. C.; Bruschi, M.; Le Gall, J. *Biochem. Biophys. Res. Commun.* **1978**, *82*, 451.
(28) Wang, V. C. C.; Can, M.; Pierce, E.; Ragsdale, S. W.; Armstrong, F. A. *J. Am. Chem. Soc.* **2013**, *135*, 2198.
(29) Kavan, L.; Grätzel, M.; Rathouský, J.; Zukalb, A. *J. Electrochem. Soc.* **1996**, *143*, 394.
(30) Fabregat-Santiago, F.; Mora-Seró, I.; Garcia-Belmonte, G.; Bisquert, J. *J. Phys. Chem. B* **2003**, *107*, 758.
(31) Bard, A. J.; Faulkner, L. R. *Electrochemical Methods: Fundamentals and Applications*, 2nd ed.; John Wiley & Sons Inc.: New York, 2001; Vol. 7.
(32) Boschloo, G.; Fitzmaurice, D. *J. Electrochem. Soc.* **2000**, *147*, 1117.
(33) Beranek, R. *Adv. Phys. Chem.* **2011**, 786759.
(34) Lee, M. S.; Cheon, I. C.; Kim, Y. I. *Bull. Korean Chem. Soc.* **2003**, *24*, 1155.
(35) Walter, M. G.; Warren, E. L.; McKone, J. R.; Boettcher, S. W.; Mi, Q.; Santori, E. A.; Lewis, N. S. *Chem. Rev.* **2010**, *110*, 6446.